Available online at www.sciencedirect.com

ScienceDirect

Procedia Engineering 173 (2017) 101 – 108

Procedia Engineering

www.elsevier.com/locate/procedia

11th International Symposium on Plasticity and Impact Mechanics, Implast 2016

Preliminary assessment of the possibilities of the Particle Finite Element Method in the numerical simulation of bird impact on aeronautical structures

M. L. Cerquaglia[a,*], G. Deliége[a], R. Boman[a], J.P. Ponthot[a]

[a] *University of Liège, Allée de la Découverte 9, Liège 4000, Belgium*

Abstract

As well known, in the analysis of bird impact events the bird is often reduced, even experimentally, to a surrogate projectile modeled as a weakly compressible fluid (typically a mixture of water and air) [15]. From a numerical standpoint, the presence of a free surface and the strong interaction with the aircraft structures represent a limit for traditional computational fluid dynamics methods based on an Eulerian grid. On the other hand, classical Lagrangian methods cannot cope with the extremely large deformations experienced by the projectile during the impact. The Particle Finite Element Method (PFEM) [6,11] is a Lagrangian particle method that can account for very large deformations, preserving the robustness and generality of the finite element method, and thus owning a key advantage over other approaches, e.g. Smoothed Particle Hydrodynamics (SPH) [9], usually cursed with consistency and stability issues [1,10]. To assess the possibilities of the method in the context of bird impact, theoretical analyses are initially performed based on the impact of a water jet on a rigid surface. Then, the influence of the geometry of a more realistic projectile is analyzed and the capability of the method to take into account separation and fragmentation is highlighted.

Peer-review under responsibility of the organizing committee of Implast 2016

Keywords: Impact; bird strike; numerical simulation; particle methods; PFEM

1. Introduction

In the last decades the advancements in numerical simulation techniques together with the necessity to improve aircraft performance without excessively increasing costs have made numerical methods an essential tool both in design and certification phases of aircraft components. When it comes to bird strike, the most difficult task from a numerical standpoint is the modeling of the bird, which undergoes extremely large deformations. Moreover, when high velocity impact is concerned the bird behaves like a slightly compressible fluid rather than like a solid, as discussed by Wilbeck [15]. Thus, the use of classical approaches like Finite Elements becomes cumbersome, and in practice some artifacts have to be introduced, often leading to a loss of generality and robustness. Moreover, since explicit time integration is usually employed, the presence of distorted elements would lead to a reduction in the

* Corresponding author. Tel.: +32-(0)4-366-9591.
E-mail address: marcolucio.cerquaglia@ulg.ac.be

Peer-review under responsibility of the organizing committee of Implast 2016
doi:10.1016/j.proeng.2016.12.043

time step size, degrading the computational efficiency. As an alternative to Finite Elements, the Smoothed Particle Hydrodynamics (SPH) [9] is often employed for the simulation of bird strike. SPH is a Lagrangian meshless method that can naturally account for extremely large deformations. Unfortunately this method is cursed with consistency and stability issues [1,10] that can sometimes compromise the entire simulation. Moreover, it is usually more expensive than Finite Element approaches (see e.g. [12]). The Particle Finite Element Method (PFEM), initially introduced in the field of civil engineering [6,11], has proven as a powerful method to solve complex free-surface fluid-structure interaction. The key idea of the method is the use of classical Finite Elements combined with a very fast remeshing procedure that allows the treatment of extremely large deformations, including separation and fragmentation. In this work a preliminary assessment of this method in the framework of bird strike is proposed. First of all, a short description of the PFEM is given, then the method is tested on the problem of a water jet impacting a rigid surface and on a more realistic bird impact, again on a rigid surface. Results are compared to available theoretical and experimental data. Finally, the capabilities of the method to take into account separation and fragmentation are highlighted in a last example and then some conclusions are drawn. It is worth underlining that in this work the bird is modeled as an *incompressible* fluid and that all the examples are *two dimensional*.

2. The PFEM

In the PFEM the fluid is discretized using a set of points, hereafter referred to as *particles*, which actually represent material points of the body. In order to evaluate the forces acting on each particle, a new mesh is built at each time step from the entire set of particles using a Delaunay triangulation combined with the so-called α*-shape* technique [4]. This allows a fast evaluation of nodal connectivity even when the total number of particles becomes very large [5]. Classical Finite Element (FE) shape functions can then be defined on this new mesh to solve the corresponding weak form of the governing equations (see Section 2.1).
Given a set of particles, the main steps within one time iteration can be summarized as follows:

1. define the particle connectivity through a Delaunay triangulation;
2. identify the domain boundaries using the α*-shape* technique;
3. solve the governing equations making use of *linear* FE shape functions;
4. use the solution obtained from the previous step to update the particle positions.

In the following, several aspects of the implementation are omitted. For a complete description of the method, the reader is referred e.g. to Idelsohn *et al.* [6] or Oñate *et al.* [11]. Finally, it is important to note that the present work focuses on two-dimensional cases.

2.1. Governing equations and weak form

At a given time t, and in the current configuration $\boldsymbol{x}$, the incompressible Navier-Stokes equations read:

$$\rho \frac{Du_i}{Dt} = -\frac{\partial p}{\partial x_i} + \mu \frac{\partial}{\partial x_j}\left(\frac{\partial u_i}{\partial x_j} + \frac{\partial u_j}{\partial x_i}\right) + \rho b_i \quad \text{in} \quad \Omega, \tag{1}$$

$$\frac{\partial u_i}{\partial x_i} = 0 \quad \text{in} \quad \Omega, \tag{2}$$

where $D(\cdot)/Dt$ is the Lagrangian, or material, derivative of the quantity $(\cdot)$, Ω is the volume occupied by the continuum in the current configuration, $\rho(\boldsymbol{x}, t)$ is the current density, $\mu(\boldsymbol{x}, t)$ is the dynamic viscosity, $\boldsymbol{u} = \boldsymbol{u}(\boldsymbol{x}, t)$ is the velocity vector, $p(\boldsymbol{x}, t)$ is the pressure, and $\rho\, \boldsymbol{b}(\boldsymbol{x}, t)$ is a body force, such as gravity for instance.
These equations have to be complemented with Dirichlet and Neumann boundary conditions:

$$\boldsymbol{u}(\boldsymbol{x}, t) = \bar{\boldsymbol{u}}(\boldsymbol{x}, t) \quad \forall \boldsymbol{x} \in \Gamma_D, \tag{3}$$

$$\boldsymbol{\sigma}(\boldsymbol{x}, t) \cdot \boldsymbol{n} = \bar{\boldsymbol{t}}(\boldsymbol{x}, t) \quad \forall \boldsymbol{x} \in \Gamma_N, \tag{4}$$

where $\bar{\boldsymbol{u}}(\boldsymbol{x},t)$ and $\bar{\boldsymbol{t}}(\boldsymbol{x},t)$ are imposed velocities and surface tractions respectively, $\boldsymbol{\sigma} = \boldsymbol{\sigma}(\boldsymbol{x},t)$ is the Cauchy stress tensor, $\boldsymbol{n}$ denotes the unit outward normal to the boundary, $\Gamma_D \cup \Gamma_N = \partial\Omega$, where $\partial\Omega$ is the boundary of the current volume Ω, and $\Gamma_D \cap \Gamma_N = \emptyset$.
Consider the following spaces for trial and test functions

$$\begin{aligned} S &= \left\{\boldsymbol{u} \in \mathbf{H}^1(\Omega) | \boldsymbol{u} = \bar{\boldsymbol{u}} \quad \text{on} \quad \Gamma_D\right\}, \\ S_0 &= \left\{\boldsymbol{w} \in \mathbf{H}^1(\Omega) | \boldsymbol{w} = \boldsymbol{0} \quad \text{on} \quad \Gamma_D\right\}, \\ Q &= \left\{q \in H^1(\Omega)\right\}, \end{aligned}$$

where $H^1(\Omega)$ is the space of square integrable functions with square integrable first derivatives over the domain Ω. The weak form of Equations (1) and (2) can be established by multiplying Equation (1) by a vector test function $\boldsymbol{w} \in S_0$ and Equation (2) by a scalar test function $q \in Q$. Integrating over the current volume and using Green's theorem, the weak form finally reads:
find $\boldsymbol{u} \in S \times [0,T]$ and $p \in Q \times [0,T]$ such that

$$\begin{aligned} \int_\Omega \rho \frac{Du_i}{Dt} w_i \, \mathrm{d}\Omega = \int_\Omega p \, \delta_{ij} \frac{\partial w_i}{\partial x_j} \, \mathrm{d}\Omega - \int_\Omega \mu \left(\frac{\partial u_i}{\partial x_j}\frac{\partial w_i}{\partial x_j} + \frac{\partial u_j}{\partial x_i}\frac{\partial w_i}{\partial x_j} \right) \mathrm{d}\Omega \\ + \int_\Omega \rho \, b_i w_i \, \mathrm{d}\Omega + \int_{\Gamma_N} \bar{t}_i w_i \, \mathrm{d}\Gamma_N \quad \forall \boldsymbol{w} \in S_0, \end{aligned} \tag{5}$$

$$\int_\Omega \frac{\partial u_i}{\partial x_i} q \, \mathrm{d}\Omega = 0 \quad \forall q \in Q. \tag{6}$$

To circumvent the Ladyzhenskaya-Babuška-Brezzi (LBB) condition a Petrov-Galerkin pressure stabilization procedure has been preferred over a fractional step method as it shows better mass conservation properties, as demonstrated by Cremonesi *et al.* [3]. The stabilized version of Equation (6) then reads

$$\begin{aligned} -\int_\Omega \frac{\partial u_i}{\partial x_i} q \, \mathrm{d}\Omega + \sum_{e=1}^{N_{el}} \int_{\Omega_e} \tau^e_{\mathrm{PSPG}} \frac{1}{\rho} \frac{\partial q}{\partial x_i} \left(\rho \frac{Du_i}{Dt} + \frac{\partial p}{\partial x_i} \right. \\ \left. -\mu \frac{\partial}{\partial x_j} \left(\frac{\partial u_i}{\partial x_j} + \frac{\partial u_j}{\partial x_i} \right) - \rho b_i \right) \mathrm{d}\Omega_e = 0 \quad \forall q \in Q, \end{aligned} \tag{7}$$

where N_{el} is the total number of elements. The parameter τ^e_{PSPG} can be computed as

$$\tau^e_{\mathrm{PSPG}} = \frac{\tilde{h}^e}{2\|\tilde{\boldsymbol{U}}\|}, \tag{8}$$

where $\tilde{h}^e$ is defined as the diameter of the circle which is area-equivalent to element e and $\tilde{\boldsymbol{U}}$ is a global user-defined scaling velocity [14].

2.2. Time integration

Time integration is performed using an unconditionally-stable implicit Euler scheme. Positions at time t^{n+1} are computed as

$$\boldsymbol{x}^{n+1} = \boldsymbol{x}^n + \boldsymbol{v}^{n+1}\Delta t, \tag{9}$$

which leads to the system of fully discrete equations

$$\begin{bmatrix} \frac{1}{\Delta t}\mathbf{M}^{n+1} + \mathbf{K}^{n+1} & \mathbf{D}^{Tn+1} \\ \frac{1}{\Delta t}\mathbf{C}^{n+1} - \mathbf{D}^{n+1} & \mathbf{L}^{n+1} \end{bmatrix} \begin{Bmatrix} \boldsymbol{v}^{n+1} \\ \boldsymbol{p}^{n+1} \end{Bmatrix} = \begin{Bmatrix} \boldsymbol{f}^{n+1} + \frac{1}{\Delta t}\mathbf{M}^{n+1}\boldsymbol{v}^n \\ \boldsymbol{h}^{n+1} + \frac{1}{\Delta t}\mathbf{C}^{n+1}\boldsymbol{v}^n \end{Bmatrix}. \tag{10}$$

where $\mathbf{M}$ is the mass matrix (that can be lumped if needed), $\mathbf{K}$ the matrix containing the viscous terms, $\mathbf{D}$ the discrete version of the divergence operator, and $\boldsymbol{f}$ a vector containing the contribution of body forces and surface tractions, i.e. the applied forces. $\mathbf{C}$ represents a dynamic stabilization term and $\mathbf{L}$ is the discretized version of the Laplacian operator. A Picard algorithm is used to solve the non linear system (10). For all the studies presented in this work one or two non linear iterations were enough to reach convergence.

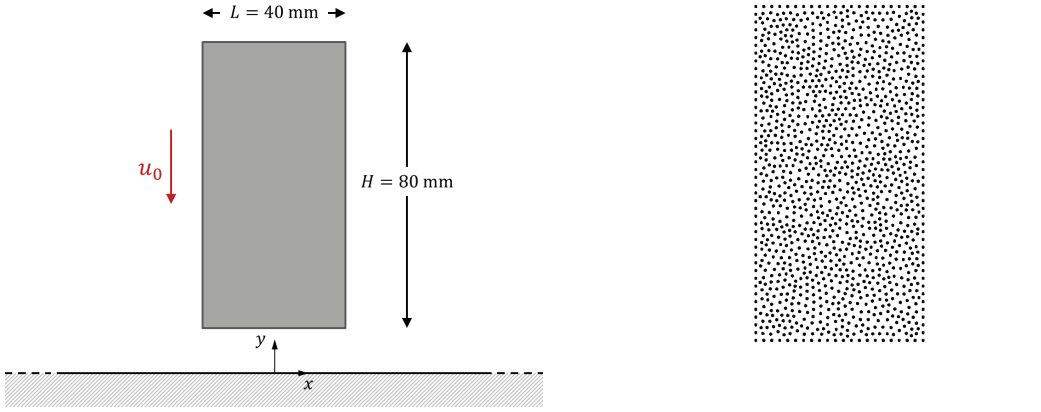

(a) Impact of a water jet on a rigid flat plate. Problem set.

(b) Discretization chosen for the simulations

Fig. 1: Impact of a water jet on a rigid flat plate.

3. Water jet impacting on a rigid flat plate

The impact of a water jet on a rigid flat plate is analyzed in the first place. This problem has already been investigated in the past, in the stationary case, both from a theoretical and experimental viewpoint, for example by Schach [13] and Liu *et al.* [8], and represents a natural starting point for our analysis. In this case however, since a fully Lagrangian approach is employed, the impact of a *finite* jet, whose dimensions are given in Fig. 1(a), is considered.

Some attention should be drawn to the way the total impact time, T, and the time step, Δt, are chosen. The total time T is taken of the order of the time employed by the whole jet to collapse against the rigid wall, that is:

$$T \simeq \frac{H}{u_0}.$$

Since no CFL condition has to be verified, the time step Δt is estimated only based on contact detection requirements. In this work it has been chosen as one third of the time needed to cross one element moving at velocity u_0, i.e.:

$$\Delta t = \frac{1}{3}\frac{h}{u_0},$$

where h is the average element size. These considerations are valid for all the other studies presented in this work.

3.1. *Impact at* $u_0 = 10$ m/s

Some preliminary analyses are conducted at an impact speed $u_0 = 10$ m/s. This value has been chosen arbitrarily. First, a mesh convergence study is performed in order to choose the right discretization. The results are shown in Fig. 2(a) and 2(b), where the pressure evolution at the center of the plate is regarded as the quantity of interest. Note that in this analysis the same time step, corresponding to the finest discretization i.e. $\Delta t = 2 \times 10^{-5}$ s, has been used for all the simulations. A discretization corresponding to 10 particles along the half width, $L/2$, is chosen for further studies. The resulting mesh is shown in Fig. 1(b). However, the pressure at the impact point is not the only interesting quantity: the pressure profile along the plate is also important. In his studies, Schach [13] proposes a theoretical and an experimental profile, both reported in Fig. 3(a) together with the analytical solution proposed by Liu *et al.* [8]. These results are compared to the profile obtained with the PFEM, evaluated at the middle of the simulation, i.e. $T/2$, this instant being considered as the closest to the case of a stationary jet. The agreement is fairly good, especially if one considers that a two-dimensional finite jet is analyzed instead of a three-dimensional axisymmetric stationary jet and that theoretical results are also derived under some simplifying assumptions.

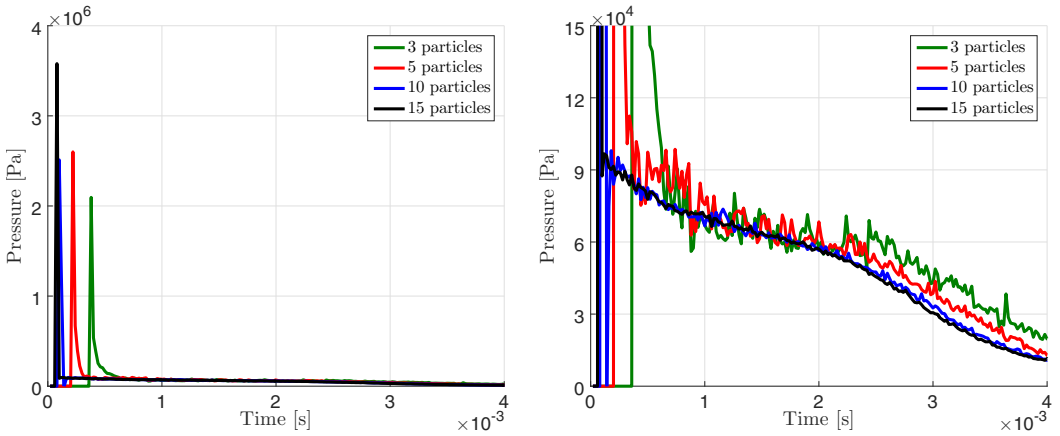

(a) Pressure evolution (b) Zoom

Fig. 2: Impact of a water jet on a rigid flat plate. Convergence analysis at $u_0 = 10$m/s: pressure evolution at the center of the plate.

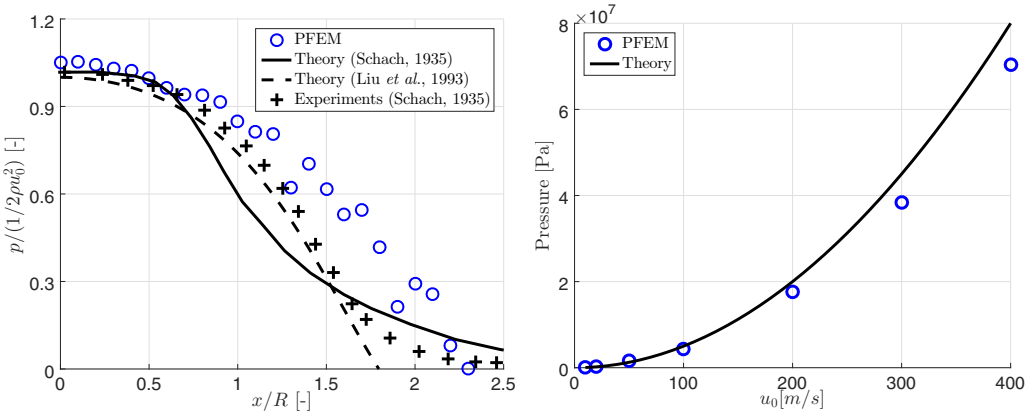

(a) Pressure profile along the plate for $u_0 = 10$ m/s. (b) Stagnation pressure for different impact speeds.

Fig. 3: Impact of a water jet on a rigid flat plate. Analysis of the pressure profile along the plate and stagnation pressure.

3.2. *Impacts between* $u_0 = 10$ m/s *and* $u_0 = 400$ m/s

In this section different impact speeds which fall into the range of interest for bird impact on aeronautical structures are considered. To evaluate the quality of the results obtained, the stagnation pressure at the center of the plate is chosen as a synthetic and sufficiently representative quantity. For a stationary jet, this pressure is equal to $p_S^{th} = \frac{1}{2}\rho u_0^2$, i.e. it grows with the square of the impact velocity. From a numerical point of view, since a steady state is never reached in this case, the stagnation pressure is computed as

$$p_S^{num} = \frac{\int_0^T p(x=0,t)\mathrm{d}t}{T}.$$

The results are shown in Fig. 3(b). The numerical solution is in very good agreement with the theoretical expectations, especially in the light of the approximation introduced by the analysis of a finite jet. Indeed, a maximum error of less than 10% has been obtained for an impact speed of 400 m/s.

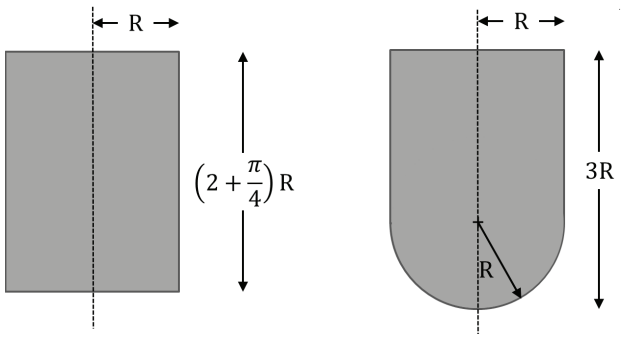

(a) Flat surface. (b) Hemispheric surface.

Fig. 4: Bird impact on a rigid flat plate. Bird models.

4. Bird impact on a rigid flat plate, $u_0 = 100$ m/s

The method is now tested on the same problem, but for a more realistic geometry, closer to the one of a real bird. The fluid is again water, which is an acceptable approximation according to the results of Wilbeck [15]. Two geometries are considered, as shown in Fig. 4. As it can be observed, the two models differ for the shape of the impacting surface, which is flat in one case (Fig. 4(a)) and hemispheric in the other (Fig. 4(b)). The dimensions for the bird have been arbitrarily chosen in the range proposed in [2], i.e. the semi-width of the body, R, has been fixed to 60 mm. For simplicity, a length of $3R$ has been chosen in the case of hemispheric impact surface (i.e. 180 mm). Conversely, in the case of flat impact surface the length is computed based on the one of the hemispheric case, so that the two projectiles have the same mass. The impact speed is also chosen to be representative of a real bird strike, i.e. $u_0 = 100$ m/s. The pressure evolution at the center of the plate is shown in Fig. 5(a). The results obtained with the two geometries are quite similar except for the amplitude of the initial peak, which is much higher in the case of a flat impact surface. This fact has already been discussed in the literature (see e.g. [7]) and could be expected somehow since the impact is less abrupt in the case of an hemispheric impactor. In Fig. 5(b) the results obtained with an hemispheric impact surface are compared to those derived experimentally by Wilbeck [15] for a similar impact speed (117 m/s). The agreement is very good, except for the amplitude of the initial peak. Nonetheless, some considerations are in order. First of all, the correct amplitude of this peak is extremely delicate to evaluate and a value of 12 times the stagnation pressure is not unphysical, as it can be found elsewhere in the literature both in numerical and experimental results (see again [7]). Moreover, in this case the analysis is limited to two dimensions and to an incompressible fluid, while experimental data result, of course, from three-dimensional tests, and from the use of slightly compressible projectiles.

5. Bird impact on a pseudo leading edge, $u_0 = 100$ m/s

As a last example, the bird model previously validated is tested for the impact on a pseudo-leading edge of an aircraft wing. Since the target is still rigid, the only purpose of this study is to prove the capabilities of the PFEM to take into account extremely large deformations and eventually the complete fragmentation of the impacting body. Indeed, the bird is often cut during the impact, either by the leading edge of a wing or by the fan blades in an engine, and this has of course important consequences on the dynamics of the impact event. Being capable to take this fact into account is thus of paramount importance. The geometry of the problem is described in Fig. 6, all the coordinates are expressed in mm. The front part of the leading edge has been constructed using a B-spline whose control points are A, B and C. The two remaining segments (in green) are just straight lines. The leading edge is discretized according to the bird discretization. The initial speed is 100 m/s. The global evolution of the impact event is shown in Fig. 7. As it can be observed the method is perfectly capable to account for extremely large deformations up to the complete separation of the bird into halves. It has to be noticed that no convergence or stability problems arose during the simulation.

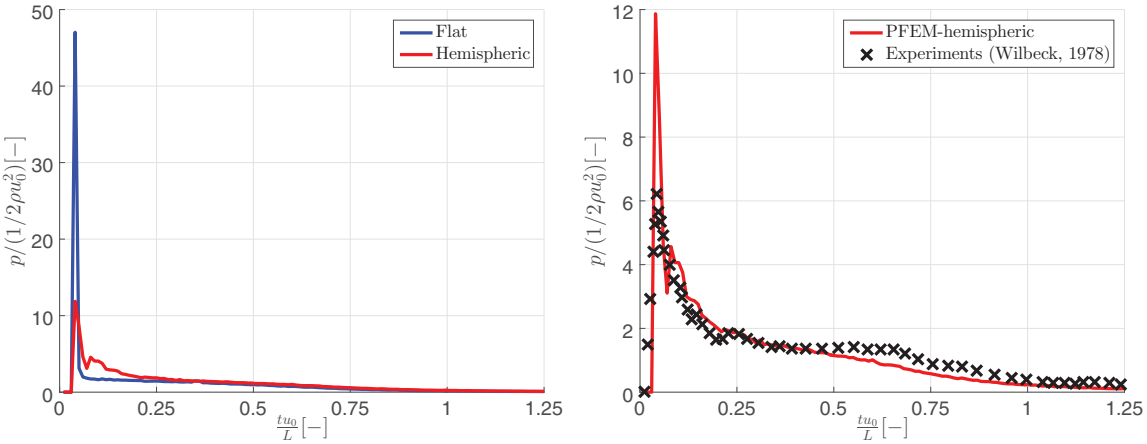

(a) Flat vs hemispheric impactor.

(b) Comparison with experimental results.

Fig. 5: Bird impact on a rigid flat plate. Pressure at the center of the plate.

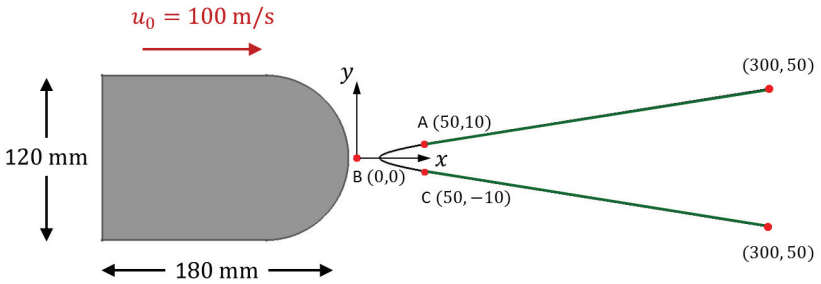

Fig. 6: Bird impact on a pseudo leading edge. Problem geometry.

6. Conclusions

A preliminary assessment of the potentialities of the PFEM for the simulation of bird strike events on aircraft structures has been performed. The method has been first validated through the analysis of the impact of a water jet on a rigid flat plate, providing good results in terms of prediction of the pressure at the impact point, the pressure profile along the plate and the stagnation pressure for a typical aircraft range of velocities. Then, a geometry closer to a real bird has been considered, confirming a good agreement with experimental results from the literature regarding the pressure evolution at the impact point. Finally it has been shown how the method can easily account for large deformations and fragmentation without incurring in any stability or convergence issue. Many assumptions were made in this first attempt to model bird impact through the PFEM (use of an incompressible fluid, two-dimensional tests, rigid targets), which make the method still unsuited for the simulation of real-life bird strike events. Nonetheless, the preliminary results presented in this work are very promising. In the future, the method should be extended to three dimensions, a compressible material should be employed, a full coupling with deformable targets should be implemented, and a rigorous analysis in terms of computational cost should be performed, in order to situate the PFEM among the other available techniques (FEM, SPH, ...).

References

[1] T. Belytschko, Y. Guo, W. K. Liu, and S. P. Xiao. A unified stability analysis of meshless particle methods. *International Journal for Numerical Methods in Engineering*, 48:1359–1400, 2000.

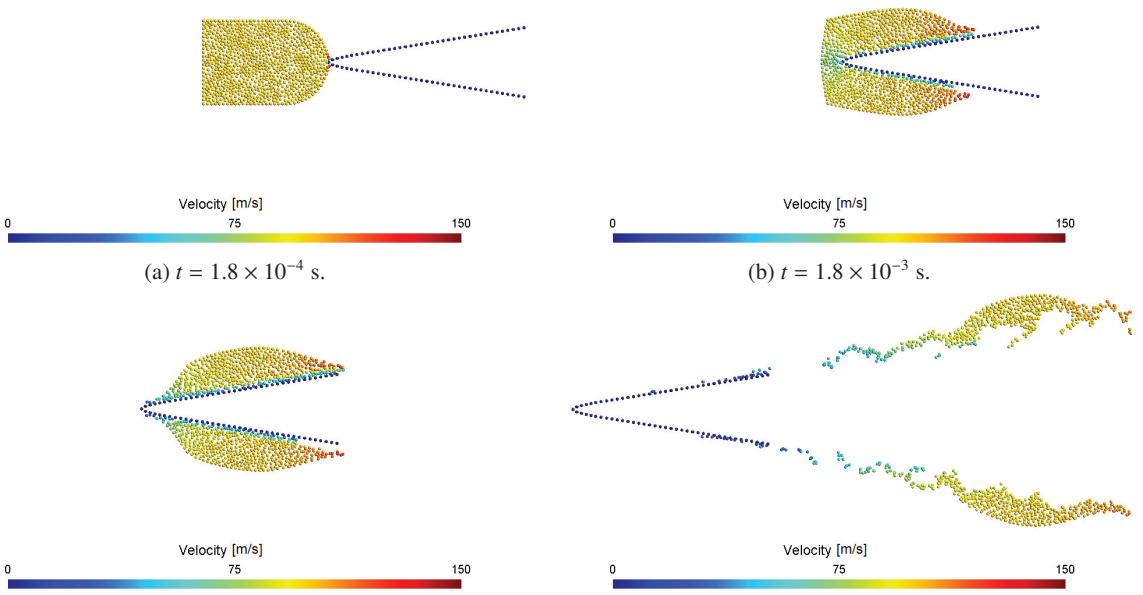

(a) $t = 1.8 \times 10^{-4}$ s. (b) $t = 1.8 \times 10^{-3}$ s.

(c) $t = 2.7 \times 10^{-3}$ s. (d) $t = 7.8 \times 10^{-3}$ s.

Fig. 7: Bird impact on a pseudo leading edge. Impact evolution.

[2] Australian Transport Safety Bureau. Research paper, the hazard posed to aircraft by birds. Technical report, Department of Transport and Regional Services, 2002.

[3] M. Cremonesi, A. Frangi, and U. Perego. A Lagrangian finite element approach for the analysis of fluid-structure interaction problems. *Int. J. Numer. Meth. Engng.*, 84(5):610–630, 2010.

[4] H. Edelsbrunner and E. P. Mücke. Three-dimensional alpha shapes. *ACM Transactions on Graphics*, 13(1):43–72, 1994.

[5] S. R. Idelsohn and E. Oñate. To mesh or not to mesh. That is the question... *Comput. Methods Appl. Mech. Engrg.*, 195:4681–4696, 2006.

[6] S. R. Idelsohn, E. Oñate, and F. Del Pin. The particle finite element method: a powerful tool to solve incompressible flows with free-surfaces and breaking waves. *Int. J. Numer. Meth. Engng.*, 61:964–989, 2004.

[7] A. Letellier. *Contribution à la modélisation des impacts d'oiseaux sur les aubes des réacteurs d'avions*. PhD thesis, (in French) Université d'Evry, 1996.

[8] X. Liu, L.A. Gabour, and J.H. Lienhard V. Stagnation-point heat transfer during impingement of laminar liquid jets: analysis including surface tension. *J. Heat Transfer*, 115(1):99–105, 1993.

[9] J. J. Monaghan and R. A. Gingold. Smoothed particle hydrodynamics: theory and application to non-spherical stars. *Monthly Notices of the Royal Astronomical Society*, 181:375–389, 1977.

[10] J. P. Morris. A study of the stability properties of smooth particles hydrodynamics. *Proceedings of the Astronomical Society of Australia*, 13: 97–102, 1996.

[11] E. Oñate, S. R. Idelsohn, F. Del Pin, and R. Aubry. The particle finite element method. An overview. *Int. J. Comput. Methods*, 1(2):267–307, 2004.

[12] A. A. Ryabov, V. I. Romanov, S. S. Kukanov, Y. N. Shmotin, and P. V. Chupin. Fan blade bird strike analysis using Lagrangian, SPH and ALE approaches. In *6th European LS-DYNA Users Conference*, 2007.

[13] W. Schach. Umlenkung eines kreisfrmigen flflssigkeitsstrahles an einer ebenen platte senkrecht ur strmungsrichtung. *Ingenieur-Archiv*, 6: 51–59, 1935.

[14] T. E. Tezduyar, S. Mittal, S. E. Ray, and R. Shih. Incompressible flow computations with stabilized bilinear and linear equal-order-interpolation velocity-pressure elements. *Comput. Methods Appl. Mech. Engrg.*, 95:221–242, 1992.

[15] J.S. Wilbeck. Impact behavior of low strength projectiles. Technical Report 77-134, Air Force Materials Laboratory, Wright-Patterson Air Force Base, Ohio 45433, July 1978.